ChemComm

COMMUNICATION

View Article Online
View Journal | View Issue

Cite this: *Chem. Commun.*, 2014, **50**, 2670

Received 26th November 2013,
Accepted 17th January 2014

DOI: 10.1039/c3cc49020c

www.rsc.org/chemcomm

Suppressing triplet state extension for highly efficient ambipolar phosphine oxide host materials in blue PHOLEDs†

Chunmiao Han,[a] Liping Zhu,[b] Fangchao Zhao,[b] Zhen Zhang,[a] Jianzhe Wang,[a]
Zhaopeng Deng,[a] Hui Xu,*[a] Jing Li,[a] Dongge Ma*[b] and Pengfei Yan[a]

A series of phosphine oxide hosts were constructed to investigate the influence of the triplet state extension in hosts on electrophosphorescence, in which DPESPOPhCz with the carbazolyl-localized triplet state endowed its blue-emitting PHOLEDs with favourable performance, including an external quantum efficiency more than 13%.

The organic semiconductors have attracted attention in recent decades owing to their unique optoelectronic characteristics and various potential and practical applications.[1] After their rapid development driven by commercial objectives, such as organic light-emitting diodes (OLEDs),[2–5] the factors constraining the further improvement of the material and device performances clearly reflect the inconsistency between the physical properties,[6] which forces people to obtain an insight into the molecular ground and excited states and establish a deep understanding of the correlations between the molecular structures and material performances. Both optical and electrical properties should be optimized when designing desired electroluminescent (EL) materials due to the involvement of electrical and energy transfer processes. However, different from electrical properties of materials constructed with explicit purposes and almost quantitative molecular design, the influencing factors for optical properties are more obscure and complicated, which encourage the continual efforts in clarifying the effect of optical properties of specific molecular structures on the EL performance.[7–8]

Recently, the electrical performance of blue phosphorescent OLEDs (PHOLEDs) has been paid much attention,[9,10] requiring both high T_1 and strong carrier injecting/transporting ability for host materials through multifunctionalization.[11–20] In this case, the accurate control of the excited states of these complicated polynary systems becomes significant.[21] Recently, we found that the negative effects on T_1 excited states from surrounding molecules can be suppressed by rationally tuning their locations.[22] In this sense, the low T_1 energy level of a conventional host CBP is ascribed to its conjugation extension by diphenylene, which can be suppressed by the two methyl groups in CDBP (Fig. 1a).[23] However, according to spin density distributions of these two hosts, the diphenylene-involved T_1 state of CBP should be another determinant. To figure out the influence of the T_1 location, a big challenge is to establish a flexible platform with similar molecular components and conjugation and different T_1 extension for the rational conclusions without other interferences, which is crucial for further designing highly efficient host materials.

In this contribution, a series of aryl phosphine oxide (APO) hosts named **DPExPOPhCzn** were designed and prepared as the combinations of hole-transporting carbazolyl and electron-transporting diphenylphosphine oxide (DPPO) bridged by diphenylether on the basis of a multi-insulating linkage strategy (Fig. 1b). The number and

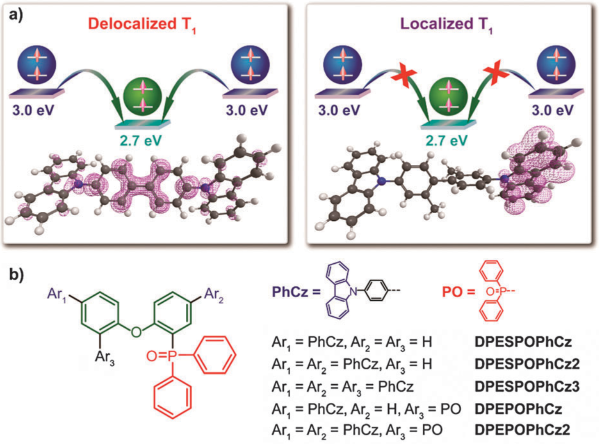

Fig. 1 (a) Potential correspondence between T_1 locations of the hosts containing low T_1 segments and their T_1 energy levels, exampled by spin density distribution of CBP (left, T_1 = 2.65 eV) and CDBP (right, T_1 = 2.99 eV); (b) chemical structures of **DPExPOPhCzn**.

---

[a] *Key Laboratory of Functional Inorganic Material Chemistry, School of Chemistry and Materials, Heilongjiang University, Ministry of Education, Harbin 150080, P. R. China. E-mail: hxu@hlju.edu.cn; Fax: +86 451 86608042*
[b] *State Key Laboratory of Polymer Physics and Chemistry, Changchun Institute of Applied Chemistry, Chinese Academy of Sciences, Changchun 130022, P. R. China. E-mail: mdg1014@ciac.jl.cn*

† Electronic supplementary information (ESI) available: Experimental details, cif file, thermal properties, DFT calculation results, CV curves and EL performance of the devices. CCDC 973794. For ESI and crystallographic data in CIF or other electronic format see DOI: 10.1039/c3cc49020c

ratio of carbazolyl and DPPO moieties were gradually adjusted to not only modulate the electrical activity, but also change the molecular geometries. Since DPPO moieties were hardly involved in T_1 states, in **DPExPOPhCzn**, two segments with different T_1 as carbazolyl (3.0 eV) and diphenylene (2.7 eV) should be considered when investigating the T_1 state variation, which just provided a flexible platform to investigate the correlation between T_1 excited state locations in these molecules and the EL performance of their corresponding PHOLEDs without interferences from other structural factors.

DPExPOPhCzn exhibited a similar absorption spectra containing three bands, corresponding to the n–π* and π–π* transitions from carbazolyl to diphenylether and the π–π* transition of DPPO (Fig. 2a). In accord with the number of functional groups, the first singlet energy levels (S_1) were slightly decreased from **DPESPOPhCz** to **DPESPOPhCz2** (Table S1, ESI†). However, it was noticed that the ternary carbazolyl in **DPESPOPhCz3** did not lead to further S_1 reduction. Simultaneously, compared with **DPESPOPhCz**, the secondary carbazolyl in **DPESPOPhCz2** and the secondary DPPO in **DPEPOPhCz** resulted in a similar S_1 decrease of ~0.06 eV, which revealed the slight influence of conjugation extension on S_1 owing to the involvement of insulating linkages such as –O– and P=O. Furthermore, the similar S_1s of **DPESPOPhCz3** and **DPEPOPhCz2** indicated that the charge transfer (CT) interaction between carbazolyl and DPPO was effectively suppressed by the *meso* linkage. Furthermore, all of the compounds exhibited UV and deep blue emissions in the same range from 340 to 500 nm with a slight bathochromic shift interval of about 10 nm. Absorption and emission spectra of **DPExPOPhCzn** in the PS or PMMA matrix further indicated their similar S_1 characteristics (Fig. S3, ESI†). Therefore, the conjugation extension was effectively suppressed by the multi-insulating linkage strategy, which was consistent with the density function theory (DFT) simulation results (Fig. S4, ESI†). Significantly, a sharp reduction of T_1 was observed for **DPESPOPhCz3** (T_1 = 2.84 eV) compared with its mono and di-substituted analogs (T_1 = 3.00 eV) due to the 0–0 transitions in their time-resolved phosphorescence spectra (Fig. 2b). Considering the similar T_1 value of **DPESPOPhCz** and **DPESPOPhCz2**, conjugation extension and more functional groups should not be the main reason for this T_1 reduction of **DPESPOPhCz3**. The situation was similar to **DPEPOPhCz2**, whose T_1 was considerably lower than that of **DPEPOPhCz**. Since **DPExPOPhCzn** were designed with two T_1 contributable carbazolyl and diphenylene groups, the T_1s of **DPESPOPhCz3** and **DPEPOPhCz2** almost in the middle of those of carbazolyl and diphenylene suggested the simultaneous contribution from these two groups to T_1 excited states, which was strongly demonstrated by DFT simulation on T_1 excited states of **DPExPOPhCzn** (Fig. 2c). The spin density distributions of T_1 states of **DPESPOPhCz**, **DPESPOPhCz2** and **DPEPOPhCz** are completely localized on carbazolyl, while diphenylene in **DPESPOPhCz3** and **DPEPOPhCz2** also makes equal contributions. In this sense, it seemed that along with the increase of molecular symmetry and electron-donating effect on diphenylene, the T_1 state extension became facile. Therefore, **DPExPOPhCzn** established a flexible platform to investigate the impact of T_1 state extension on the host performance with negligible interference from conjugation extension.

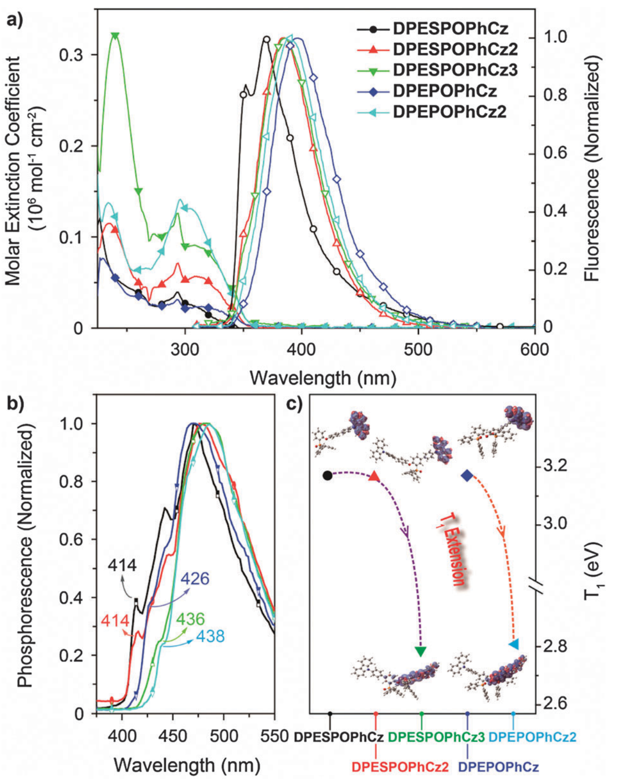

Fig. 2 (a) UV/vis absorption and fluorescence spectra of **DPExPOPhCzn** in CH_2Cl_2 (10^{-6} mol L^{-1}) at room temperature; (b) time-resolved phosphorescence spectra of **DPExPOPhCzn** in CH_2Cl_2 at 77 K after a delay of 300 μs; (c) calculated T_1 energy levels of **DPExPOPhCzn** and contours of the spin density distributions by the DFT method.

DFT simulation indicated that the increase of phenylcarbazole groups can reduce the lowest unoccupied molecular orbital (LUMO) energy level owing to the major contributions from diphenylene moieties accompanied with the elevation or preservation of the highest occupied molecular orbital (HOMO) energy level (Fig. S4, ESI†), which was in accord with the cyclic voltammetrical (CV) results except for the smaller differences between the experimental HOMO and LUMO data of **DPExPOPhCzn** estimated by the onset potentials of their redox peaks (Fig. S5, ESI†). Considering the predominance of three-dimensional multifunctionalization in carrier transportation, **DPESPOPhCz3** and **DPEPOPhCz2** should be superior in electrical performance compared with their analogs containing less carbazolyl groups. IV characteristics of single-carrier transporting devices further indicated the much more balanced charge transportation in **DPESPOPhCzn** (n = 2 and 3) and **DPEPOPhCz2** than those of **DPExPOPhCz** (Fig. S6, ESI†).

To validate the influence of T_1 state extension on the EL performance of the host materials, the blue PHOLEDs with a conventional device configuration of ITO|MoO_3 (10 nm)|NPB (70 nm)|TCTA (5 nm)|**DPExPOPhCzn**:FIrpic (15%, 20 nm)|TPBi (35 nm)|LiF (1 nm)|Al were fabricated, namely **PA–PE**, respectively. **DPESPOPhCz** endowed **PA** with the lowest driving voltages of 3.1 V for onset, 4.1 V at 100 cd m^{-2} for display and 5.7 V at 1000 cd m^{-2} for lighting (Fig. 3a and Table S2, ESI†). Other devices also had similar turn-on voltages of 3.1 V for **PB** and **PD** and 3.3 V for **PC** and **PE**, which was consistent with DFT simulation results. The energy level scheme of the devices further indicated the analogous direct charge capture process for the exciton confinement on FIrpic due to the similar FMO energy gaps between hosts and guest (Scheme S1, ESI†).

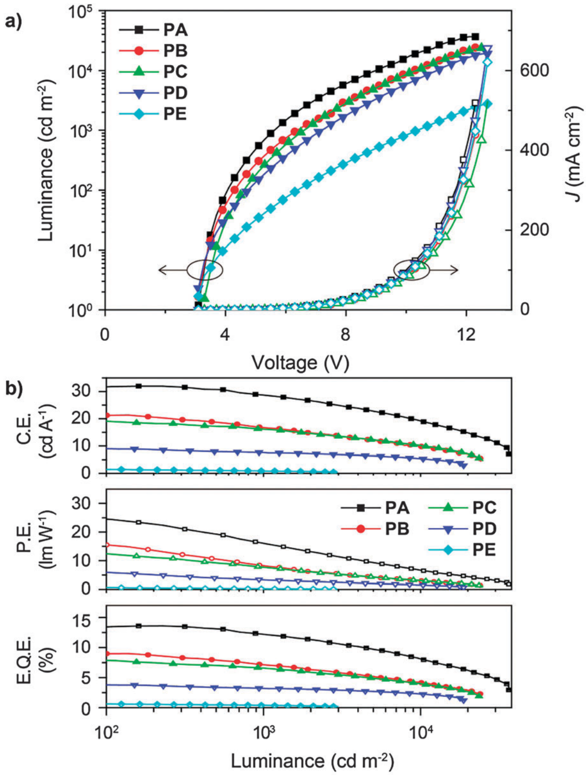

Fig. 3 Brightness–current density (*J*)–voltage curves (a) and efficiency *vs.* luminance characteristics of **PA–PE** (b).

However, at the practical luminance, the driving voltages were gradually increased, especially for **PC** and **PE**. Obviously, because of the similar volt–ampere characteristics of these devices, the remarkably higher driving voltages of **PC** and **PE** can be ascribed to the less efficient exciton confinement on FIrpic through energy transfer from **DPESPOPhCz3** and **DPEPOPhCz2** rather than the carrier injection and transportation.

The efficiency curves of these devices directly evidenced the influence of the T_1 excited state extension on exciton harvesting (Fig. 3b). **DPESPOPhCz** endowed **PA** with the highest efficiencies with 32.0 cd A^{-1} for current efficiency (C.E.), 25.1 lm W^{-1} for power efficiency (P.E.) and 13.6% for external quantum efficiency (E.Q.E.) among these devices, which were favourable among the best results of FIrpic-based devices reported so far (Table S2, ESI†). Significantly, **PA** showed an extremely low efficiency roll-off along with the increase in luminance, which were negligible for C.E. and E.Q.E. and only 3% for P.E. at 100 cd m^{-2} and as low as 11, 37 and 11% for C.E., P.E. and E.Q.E., respectively, at 1000 cd m^{-2}. Although **PB** achieved the highest P.E. of 27.7 lm W^{-1}, its C.E. and E.Q.E. were lower than those of **PA**, accompanied with the much less efficiency roll-offs at high luminance. It was noticeable that compared with **PA**, the maximum efficiencies of **PC** were dramatically reduced ~25%, while its efficiency roll-offs were as much as 23, 48 and 23% at 100 cd m^{-2} and 34, 68 and 36% at 1000 cd m^{-2}, respectively. The situation for **PD** and **PE** was similar that the maximum efficiencies of **PD** were almost 4 times of those of **PE**, accompanied with the much less efficiency roll-offs. Obviously, the T_1 state extension of **DPESPOPhCz3** and **DPEPOPhCz2** should be one of the main reasons for the much worse EL performance of **PC** and **PE**, ascribed to low host–guest energy transfer efficiencies and worse quenching effects due to increased collisional probability between T_1 exciton and other particles. The latter was evidenced by a significant decrease in the nonexponential decay time of FIrpic doped in **DPESPOPhCz3** and **DPEPOPhCz2** films (8%), compared with their analogues (Fig. S8, ESI†).

In summary, the influence of the T_1 excited state extension in host materials on their EL performance was investigated through a series of APO hosts with the same building blocks to get rid of the interferences from other structural factors. **DPESPOPhCz** with the carbazolyl-localized T_1 state endowed its blue PHOLEDs with favourable EL performance, with an E.Q.E. more than 13% and well-controlled efficiency reduction. It was seen that the T_1 state extension remarkably reduced the EL efficiencies and worsened the efficiency roll-offs due to the resulting lower T_1 energy level and the increased probability of collisional quenching effects, indicating the significance of the T_1 state location when designing high-energy-gap host materials.

CH, LZ and FZ contributed equally to this work. This project was financially supported by NSFC (61176020 and 51373050), New Century Excellent Talents Supporting Program of MOE (NCET-12-0706), Program for Innovative Research Team in University (MOE) (IRT-1237), New Key Project of MOE (212039) and New Century Excellent Talents Developing Program of Heilongjiang Province (1252-NCET-005).

Notes and references

1 W. Huang, B. Mi and Z. Gao, *Organic Electronics*, Science Press, Beijing, 2011.
2 C. W. Tang and S. A. VanSlyke, *Appl. Phys. Lett.*, 1987, **51**, 913–915.
3 J. H. Burroughes, D. D. C. Bradley, A. R. Brown, R. N. Marks, K. Mackay, R. H. Friend, P. L. Burns and A. B. Holmes, *Nature*, 1990, **347**, 539–541.
4 J. Kido, M. Kimura and K. Nagai, *Science*, 1995, **267**, 1332–1334.
5 M. A. McCarthy, B. Liu, E. P. Donoghue, I. Kravchenko, D. Y. Kim, F. So and A. G. Rinzler, *Science*, 2011, **332**, 570–573.
6 S. Reineke, F. Lindner, G. Schwartz, N. Seidler, K. Walzer, B. Lussem and K. Leo, *Nature*, 2009, **459**, 234–238.
7 G. M. Farinola and R. Ragni, *Chem. Soc. Rev.*, 2011, **40**, 3467–3482.
8 X.-H. Zhu, J. Peng, Y. Cao and J. Roncali, *Chem. Soc. Rev.*, 2011, **40**, 3509–3524.
9 L. Xiao, Z. Chen, B. Qu, J. Luo, S. Kong, Q. Gong and J. Kido, *Adv. Mater.*, 2011, **23**, 926–952.
10 Y. Tao, C. Yang and J. Qin, *Chem. Soc. Rev.*, 2011, **40**, 2943–2970.
11 D. Hu, F. Shen, H. Liu, P. Lu, Y. Lv, D. Liu and Y. Ma, *Chem. Commun.*, 2012, **48**, 3015–3017.
12 C. S. Oh, C. W. Lee and J. Y. Lee, *Chem. Commun.*, 2013, **49**, 3875–3877.
13 E. Mondal, W.-Y. Hung, H.-C. Dai and K.-T. Wong, *Adv. Funct. Mater.*, 2013, **23**, 3096–3105.
14 K. S. Yook and J. Y. Lee, *Adv. Mater.*, 2012, **24**, 3169–3190.
15 W. Yang, Z. Zhang, C. Han, Z. Zhang, H. Xu, P. Yan, Y. Zhao and S. Liu, *Chem. Commun.*, 2013, **49**, 2822–2824.
16 S. O. Jeon and J. Y. Lee, *J. Mater. Chem.*, 2012, **22**, 4233–4243.
17 D. Yu, F. Zhao, C. Han, H. Xu, J. Li, Z. Zhang, Z. Deng, D. Ma and P. Yan, *Adv. Mater.*, 2012, **24**, 509–514.
18 C. Han, Z. Zhang, H. Xu, J. Li, G. Xie, R. Chen, Y. Zhao and W. Huang, *Angew. Chem., Int. Ed.*, 2012, **51**, 10104–10108.
19 C. Han, Z. Zhang, H. Xu, S. Yue, J. Li, P. Yan, Z. Deng, Y. Zhao, P. Yan and S. Liu, *J. Am. Chem. Soc.*, 2012, **134**, 19179–19188.
20 H. Sasabe, Y.-J. Pu, K. Nakayama and J. Kido, *Chem. Commun.*, 2009, 6655–6657.
21 S. Gong, X. He, Y. Chen, Z. Jiang, C. Zhong, D. Ma, J. Qin and C. Yang, *J. Mater. Chem.*, 2012, **22**, 2894–2899.
22 Z. Zhang, Z. Zhang, R. Chen, J. Jia, C. Han, C. Zheng, H. Xu, D. Yu, Y. Zhao, P. Yan, S. Liu and W. Huang, *Chem.–Eur. J.*, 2013, **19**, 9549–9561.
23 S. Tokito, T. Iijima, Y. Suzuri, H. Kita, T. Tsuzuki and F. Sato, *Appl. Phys. Lett.*, 2003, **83**, 569–571.